Geomorphology 319 (2018) 62–77

Contents lists available at ScienceDirect

Geomorphology

journal homepage: www.elsevier.com/locate/geomorph

# Controls on strath terrace formation and evolution: The lower Guadiana River, Pulo do Lobo, Portugal

Jose A. Ortega-Becerril [a,*], Guillermina Garzón [b], Rosa Tejero [b]

[a] Dpto. de Geología y Geoquímica, Universidad Autónoma de Madrid, Madrid 28049, Spain
[b] Dpto. Geodinámica, Facultad de Geología, Universidad Complutense de Madrid, Madrid 28040, Spain

ARTICLE INFO

*Article history:*
Received 1 March 2018
Received in revised form 17 July 2018
Accepted 18 July 2018
Available online 20 July 2018

*Keywords:*
Strath terrace
Knickpoint
Inner channel
Bedrock rivers
Guadiana canyon

ABSTRACT

The lower Guadiana River carves a wide canyon in the Variscan metamorphic rocks of the SW Iberian Peninsula and presents an exceptionally homogeneous and well-preserved case of a strath terrace (ST) some 40 km long and 400 m wide. The rocky surface or strath shows different characteristics and development stages. Upstream, the lateral erosion level forms a flooded riverbed, or submerged strath, that gradually rises above the thalweg and develops into an active floodplain. Downstream, below the 15 m high Pulo do Lobo waterfall, the strath is incised by an inner canyon that forms a terrace on both sides. The inner channel increasingly widens and the ST loses its longitudinal continuity, yet remains prone to flooding during extraordinary magnitude floods. To assess the factors controlling the formation of this ST, we examined the roles of key drivers of ST formation: lithological hardness, tectonic structures and climate change, using cosmogenic data to create a chronologic context. The ST developed favoured by a monotonous succession of phyllites, as shown by Schmidt hammer resistance data, and interbedded more resistant quartz veins do not significantly alter its flat configuration. Variscan structures and measured joints determine the main orientation of the river and control the drainage network pattern. The intersection of the N—S and NE-SW fractures promotes a wavy surface due to three-dimensional minor fold trains that act as discontinuities and play an important role in ST erosion through quarrying and plucking. However, we detected no evidence of ST deformation attributable to recent or Late Cenozoic tectonic activity.

The upstream active riverbed progressively changes downstream into an ST. This implies that Be radiometric ages obtained at Pulo do Lobo may not represent the ST's genetic age but rather the time of dismantling of its alluvial or sedimentary cover. This means the strath surface formed prior to its cosmogenic age and was therefore controlled by a higher base level, indicating a higher sea level than the current one, given the downstream area studied. The Quaternary sea level fluctuations show records of only a few meters above the current level. Instead, the sea level low stand maintains an average depth of −60 m, reaching −140 m during the last glacial period. This low base level context could justify the strong incision of the inner channel within the ST, but not the age of strath surface genesis and expansion and thus this surface should have evolved previously. The highest possible sea level stand corresponds to the Pliocene transgression, which reached an elevation of 120 m in the region, covering Miocene paleorelief. The mouth of the Guadiana River at that time resembled a fluvio-deltaic embayment between the Algarve domain and the Guadalquivir depression, which was infilled with fluvial deposits at the end of the transgression. Collectively, these data suggest that cosmogenic dating would define the time of exhumation of this Pliocene sedimentary cover.

Despite great variation of the ST ages, estimated incision rates at the knickpoint area are consistent with the total entrenchment of the Pulo do Lobo fall, especially if we consider that data correspond to an active erosion site. Highest erosion rates were found for the pothole area compared to those obtained for the higher ST surface. Radiometric ages correspond to the period of lowest Quaternary sea level and during which headward erosion would have been very active in the inner channel. The waterfall area shows more resistant lithology in its concentrated quartz veins, but this effect is inconspicuous at the ST surface. The regular gradient of 0.02 m/m and vast extension of this perched strath, linked upstream to the Guadiana riverbed, indicates a relic exhumed surface beneath its sedimentary cover. Notwithstanding the subsiding activity of the Gulf of Cádiz, the continental margin behaves as a tectonically stable block, which allows for the persistence of former morphologies in these ancient landscapes reshaped by bedrock river dissection.

© 2018 Elsevier B.V. All rights reserved.

* Corresponding author.
*E-mail address:* j.ortega@uam.es (J.A. Ortega-Becerril).

https://doi.org/10.1016/j.geomorph.2018.07.015
0169-555X/© 2018 Elsevier B.V. All rights reserved.

## 1. Introduction

Rivers that cut hard rocks sometimes develop rocky erosional surfaces known as straths (Bucher, 1932). Straths may either act as a flood zone or may undergo subsequent incision and become stranded to form a strath terrace (ST) (Bucher, 1932; Wohl, 2008). Because of their scarce presence relative to vast alluvial terrace systems and their difficult temporal interpretation, reports of ST have amounted only to isolated descriptions in the literature. However, the growing attention paid by scientists to bedrock rivers and their significance in incision and landscape evolution models has rekindled an interest in these landforms (e.g., Pazzaglia and Gardner, 1993; Merritts et al., 1994; Pazzaglia et al., 1998; Cheng et al., 2002; Hancock and Anderson, 2002; Wegmann and Pazzaglia, 2002; Ward et al., 2005; Garcia, 2006; Ouimet et al., 2008; Fuller et al., 2009; Goode and Wohl, 2010; Finnegan and Dietrich, 2011; Johnson and Finnegan, 2015; Collins et al., 2016; Stokes et al., 2017).

Several controls on ST formation exist (Fig. 1). Planation of these erosional surfaces was initially associated with climate-driven increased sediment flux in relation to the river's transport capacity: first, to act as a tool for abrasion to widen river channel and second, leading to aggradation and thus armoring the riverbed (Gilbert, 1877; Hancock and Anderson, 2002; Wegmann and Pazzaglia, 2002; Montgomery, 2004; Fuller et al., 2009). In reality, STs reflect a time of balance between sediment supply and discharge such that neither aggradation nor incision occurs, resulting in a graded river (Mackin, 1937; Bull, 1990).

Strath formation could reflect a pause in vertical bedrock incision or a period of increased lateral mobility of the river (Johnson and Finnegan, 2015). Temporal variation could be induced by an increased sediment supply or channel flow (e.g., Pazzaglia et al., 1998; Hancock and Anderson, 2002; Collins et al., 2016). The transition to downcutting occurs when the available energy increases, resulting in sediment remobilization and better access to the bedrock (Hancock and Anderson, 2002). Periods of valley widening are characterized by the removal of both generated and transported sediment, which keeps the sediment thickness on a forming ST relatively constant and minimizes energy variation along reaches (Wohl et al., 1999). Alternating changes in stream power (flow or slope) and/or critical power (sediment and size) lead to periods of incision if the critical power is exceeded, or to graded periods if both factors are similar such that the slope is maintained and the valley widens (Hancock and Anderson, 2002). Lithologic controls are also significant as friable bedrock favors lateral erosion and valley widening (Schanz and Montgomery, 2016), although this evolution could take place through other controls like joint and fracture orientation (Anton et al., 2015).

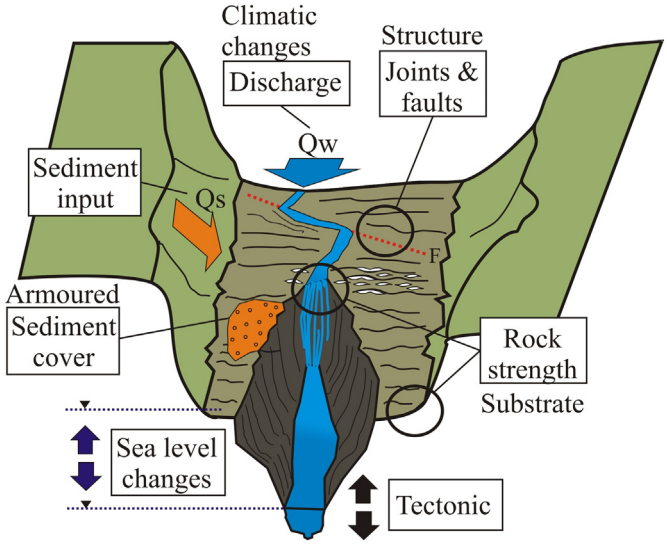


**Fig. 1.** Controls on strath terrace formation.

Here, we describe an exceptionally well-preserved case of a ST in the lower Guadiana River extending uninterrupted along its long profile from the Serpa region to the town of Mértola (see Fig. 2). The ST flanks the final reach of the Guadiana River where the river runs entrenched for 150 km through a canyon carved in the metamorphic rocks of the Iberian Massif in the SW Iberian Peninsula (Fig. 2). A topographic drop of around 100 m is produced between the regional planation surface and the valley bottom where the ST developed. This is a flood zone upstream from the Pulo do Lobo, a 15 m high waterfall, from which the river runs through an incised deep, narrow inner channel. This inner channel carved in the ST and extending through the canyon is mostly uninterrupted along some 40 km. The inner channel concentrates the entire channel flow. Then, the channel gradually widens downstream as the ST is destroyed. In this study, we address the processes that controlled the formation and development of this ST by examining how the riverbed and subsequent flat ST formed within the deep, narrow gorge of the Guadiana. This zone is ideal for this type of study as the evolution process of the ST changes downstream of the Pulo do Lobo falls, and several stages of ST formation may be observed.

According to Baker and Kale (1998), flow through deep bedrock channels is only capable of reforming the channel in times of extraordinary floods, when stream power values exceeding 100 W $m^{-2}$ are generated and confined flow via bedrock channels increases stream power, leading to the formation of pools, scablands and boulder berms. In contrast, when the width/depth ratio is large, bedrock channels develop gentler scabland morphologies dominated by polished surfaces and isolated boulders. However, Anton et al. (2015) suggest an alternative timescale and flood size for deep fluvial erosion in a densely jointed area that facilitates rapid erosion in a dam-regulated river. An example of work during extraordinary floods is provided by the Orange River (South Africa), which shows anabranching channels on a regional planation surface, the Augrabies, until a great waterfall where a deep gorge arises with an irregular bed and active sediment transport (Tooth, 2015). Confined STs of regional extension are those of the Susquehanna River (USA), that have been related to valley widening due to increased available load coinciding with high stable Cenozoic sea levels (Pazzaglia et al., 1998).

The development of STs has been mostly linked to interplay among climate, rock strength and base level changes driven by combinations of tectonic uplift, eustasy and river responses by means of capture, cut off processes, etc. (e.g., Pazzaglia and Gardner, 1993; Merritts et al., 1994; Hancock and Anderson, 2002; Stokes et al., 2017). To understand the role of both, it is important to assess the behavior of structures arising from the deformation (especially in recent times), climate changes occurring in the area, and the possible formation age of the canyon and ST. With this in mind, we here examined the main interacting factors such as lithology and structure controls on the drainage pattern, as well as age data and climate change effects at the Guadiana River mouth, 100 km downstream from the Pulo do Lobo waterfall.

The specific objectives of the present study are to understand the main controls operating in the development of the lower Guadiana River ST (Fig. 1): (1) Which factors have affected the formation of the ST? (2) Are the Guadiana River patterns and ST morphology controlled by structural discontinuities? Are the steps in the channel long profile related to individual faults? Conversely, are the steps the result of headward migration from fault areas? In the second case, we will try to assess the influence of recent tectonic events in the area. (3) Can the presence of knickpoints be linked to changes in bedrock joint characteristics and/or recent disturbances in longitudinal profile? (4) Is the climate (discharge regime and sea level changes) an important driver for ST development? (5) Is the ST developing in a continuous manner, even in periods of sea level lowering or related to periods of high sea level? (6) What is the role of the inner channel and Pulo do Lobo waterfall in ST development and preservation?

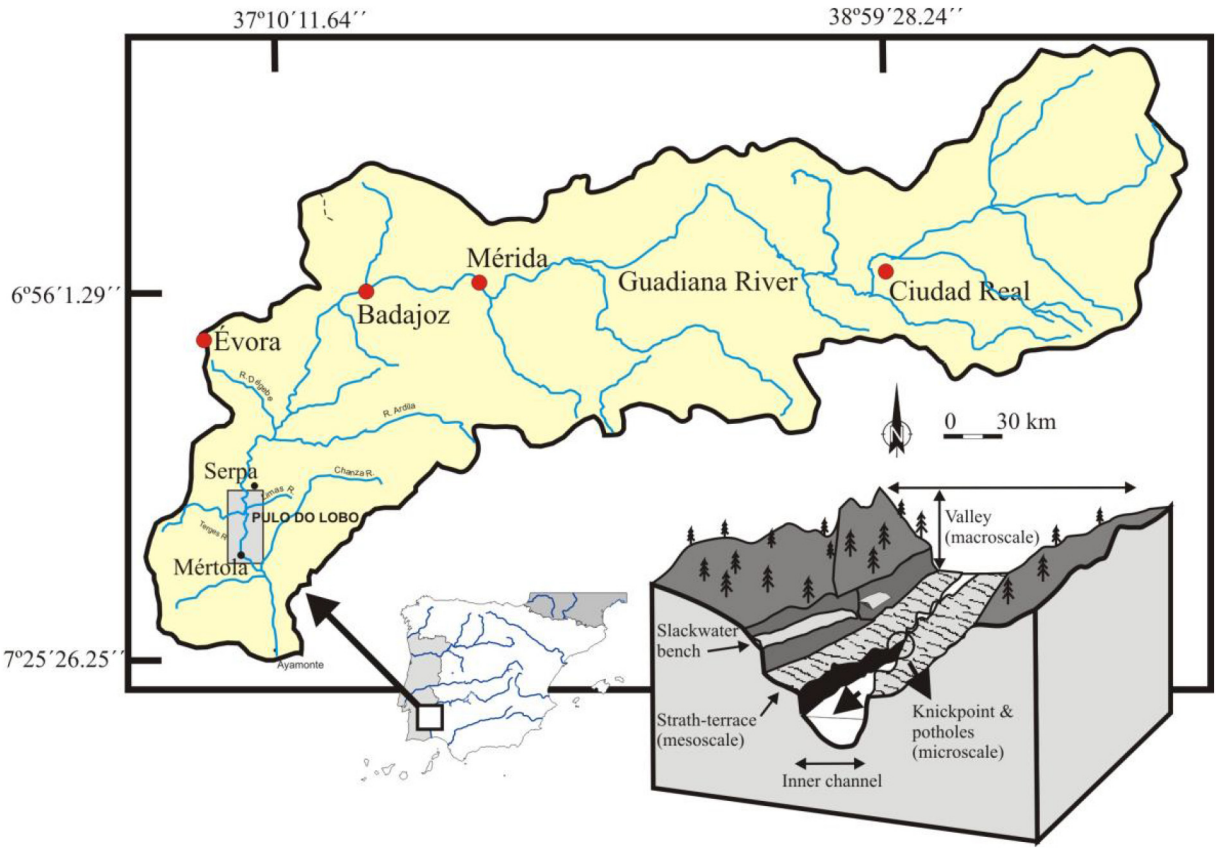


**Fig. 2.** Location of the studied portions of the Guadiana River basin and inset illustration of primary geomorphic features of the Pulo do Lobo area.

## 2. Geological and geomorphological overview of the study area

The Guadiana River forms one of the largest watersheds of the Iberian Peninsula draining towards the Atlantic Ocean. Of the Iberian rivers, it is the fourth in length (780 km) and surface area (67,733 km$^2$), yet only comes in tenth in terms of average discharge (210 m$^3$ s$^{-1}$). This is because of the basin's characteristic feature — its mountain sources rarely exceed an altitude of 1000 m, yet its mean altitude, mainly above the Variscan impervious rocks, is 450 m.

In its lower reach, the Guadiana River flows through the Paleozoic and Proterozoic rocks of the Variscan basement. It follows a roughly N—S path, cutting two main tectonostratigraphic zones of the Variscan orogen (Fig. 3A). The northern one, designated the Ossa-Morena Zone, represents an internal continental segment of the SW Iberian Variscides, limiting in the south with an external tectonic unit, the South-Portuguese Zone, through a NW trending suture. The study area occupies the northern part of the South-Portuguese Zone, where two main geological domains are recognized, the Pulo do Lobo Antiform and the Iberian Pyrite Belt (Oliveira, 1992; Ábalos et al., 2002). The Pulo do Lobo Antiform consists of several detritic and metamorphic formations recording the stratigraphy of the Upper Devonian (Fig. 3B). These formations are composed of highly sheared phyllites, greywackes and quartzites with minor intercalations of metavolcanic rocks. A typical feature of this unit is the widespread occurrence of quartz veins, generated in the outer stretched arc of folds. It is at this formation, that the ST is developed. Variscan structures arise from several stages of deformation and developed a deformation characterized by folds, thrusts, shear bands and associated foliations and tectonic banding.

The coastal plain overlies Mesozoic and end-Cenozoic materials that culminate with the Pliocene transgression sediments deposited on a previous Miocene paleorelief (Pais et al., 2012). Coinciding approximately with today's Guadiana estuary, an inland-penetrating embayment filled by deltaic deposits (Pais et al., 2012), which later became covered with fluvial sediments (Leyva and Ramírez, 1983). Significant glacio-eustatic sea level changes at the river mouth during the Pleistocene meant drastic fluvial incision over previous units (Pais et al., 2012). Greatest incision was produced under the arid and cold conditions of the last glacial maximum (around 18 ka BP) in which the sea level reached ~120 m below its current level and up to 40 km away from the coast (Lobo et al., 2003). The last marine transgression was rapid during the Holocene, yet thereafter the sea level stabilized close to the current level in the Guadiana's estuary.

Fluvial terraces are not present along the Guadiana canyon or on the estuary reach. Only few isolated patches of gravels on the highest part of the valley slopes were attributed to terrace remnants (Feio, 1946). Upstream of the canyon, however, the Guadiana River incises in the Cenozoic Moura depression and defines four terraces flights up to 90 m high. Feio (1946) related the terrace altitudinal levels with the glacial regressive stages, although this author considered they were not controlled by eustatism because there was no connection with the coast. On the coast, only three marine beaches are present that the author related to the latest interglacial stages.

Correlating the Guadiana's terrace with other Iberian fluvial basins is difficult. The Guadiana watershed is configured by fluvial reaches incised on the Varisc substrate alternating with reaches in Cenozoic depressions. Terraces develop only in these sedimentary basins and their evolution is controlled by its bedrock outlet (Garzón et al., 2011; Garzón and Tejero, 2018). The relatively mature character of the Guadiana basins contrasts with the terrace systems of other Iberian Atlantic rivers (Garzón and Tejero, 2018), as in the case of the Tagus River, which because of its nearer sea link undergoes eustatic influence n (Cunha et al., 2005, 2016; Martins et al., 2017). As Santisteban and Schulte (2007) synthetize, river terraces in Iberian Massif show a

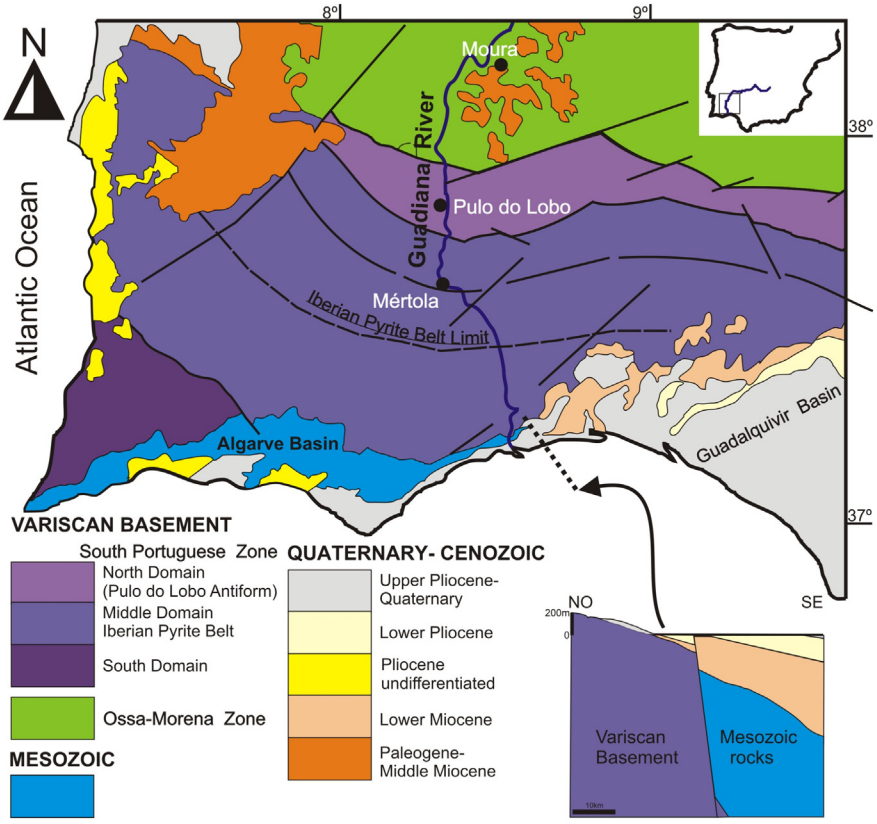


**Fig. 3.** (A) Geological map of SW Iberian Peninsula. (B) Cross section between Algarve and Guadalquivir morphotectonic domain.

complex correlation scheme due to large differences in lithological, tectonic, climate or eustatic controls.

The Guadiana mouth occurs on the eastern edge of the Algarve Basin in the contact zone with the Guadalquivir Basin, a foreland basin of the Alpine Betics Ranges. Subsidence is related to lithospheric flexure associated with active subduction at plate boundaries and the formation of the accretionary prism of the Gulf of Cádiz (Fig. 3B) (e.g., Terrinha et al., 2006). To the north, within the continental area, Alpine tectonics gave rise to Cenozoic basins. This is the case of the Moura Basin, north of the Guadiana canyon entrenchment, where an E-W thrust, the Vidigueira-Moura Fault (VMF) (Fig. 4), overlaps basement rocks on continental Cenozoic sediments (Brum da Silveira et al., 2009). Both structures, as well as other inherited faults such as the Aroche and Villanueva de los Castillejos faults, feature topographic scarps built on basement rocks (Fig. 4). Some authors have linked the Pulo do Lobo fall to a scarp associated with an active fault (Vázquez-Vílchez et al., 2015), but as shown in Fig. 6, there is no evidence of a significant displacement of the ST surface. Seismicity is relevant south of the Guadiana mouth, but is scarce in the study area. Fig. 4 shows 151 earthquakes recorded from 1980 to 2017 of magnitude >2. The maximum earthquake magnitude is 3.9 and less than ten earthquakes are located close to the Pulo do Lobo fall. Earthquake occurrence increases southwards near the Guadiana mouth and offshore (e.g., Custódio et al., 2015).

The lower reach of the Guadiana flows through a landscape dominated by a large planation surface, which indifferently cuts across and levels Paleozoic materials (Feio, 1992). The Guadiana gorge shows a distinct bedrock channel morphology with a bottom of ~400 m width, largely occupied by a strath that defines a very regular subhorizontal surface. This strath varies along its tread showing several stages of evolution (Figs. 5 and 7). Upstream, at the start of the canyon, this lateral erosion level forms a flooded riverbed, but the strath surface gradually emerges from the current thalweg and continues as a floodplain. Downstream from the Pulo do Lobo fall, it forms a true ST hanging over an inner channel widening progressively and leaving remnants of the ST perched until they finally disappear.

The strath profile traces a highly continuous subhorizontal surface, though some stretches show significant slope. In its high reach, above the knickpoint conferred by the Pulo do Lobo falls, the slope is 0.08%. Beyond this point, the strath gradually declines to a much gentler slope (0.02%) with respect to the current Guadiana River (Fig. 6). Thus, the ST becomes elevated by 15 m in the Pulo do Lobo knickpoint zone but measures >20 m at its end, downstream from Mértola. Beneath the knickpoint, the Guadiana River adopts its characteristic concave profile, with a more marked initial slope that gradually diminishes. Along the entire reach, its longitudinal profile is broken by smaller rapids (Fig. 6).

During medium to large floods, the flanking bedrock benches are covered with water and the upstream reach of the inner channel is not visible (Ortega and Garzón, 2009). Based on paleoflood deposits recorded in the canyon rock (Ortega and Garzón, 2009) and dated by $C^{14}$ AMS and $Cs^{137}$ as ranging from 3260 BP to the present, estimated discharges are 2500–4000 $m^3\ s^{-1}$ for low magnitude floods, 4000–7000 $m^3\ s^{-1}$ for medium floods (overflowing on the ST), and >7000 $m^3\ s^{-1}$ up to 11,000 $m^3\ s^{-1}$ for high magnitude floods. Stream powers (Table 1) calculated for high magnitude floods are high at 220 W $m^{-2}$, dropping to 155 W $m^{-2}$ for the limit with medium floods and to 13 W $m^{-2}$ when there is no overflow onto the ST. In this context, Holocene palaeodischarges that reached the ST were able to transport bedload and exceedingly high sediment load. The return period for overflow on the ST is four years, though this does not occur along its entire length. At Pulo do Lobo, high flow velocities and a depth of up to 19 m in the inner channel and of 7 m on the ST are reached in medium and high magnitude floods. According to Kale (2003), such floods are able to mobilize boulder-sized materials.

The ST shows no sedimentary cover, except in its final reach where fine overflow deposits related to major floods appear. This zone

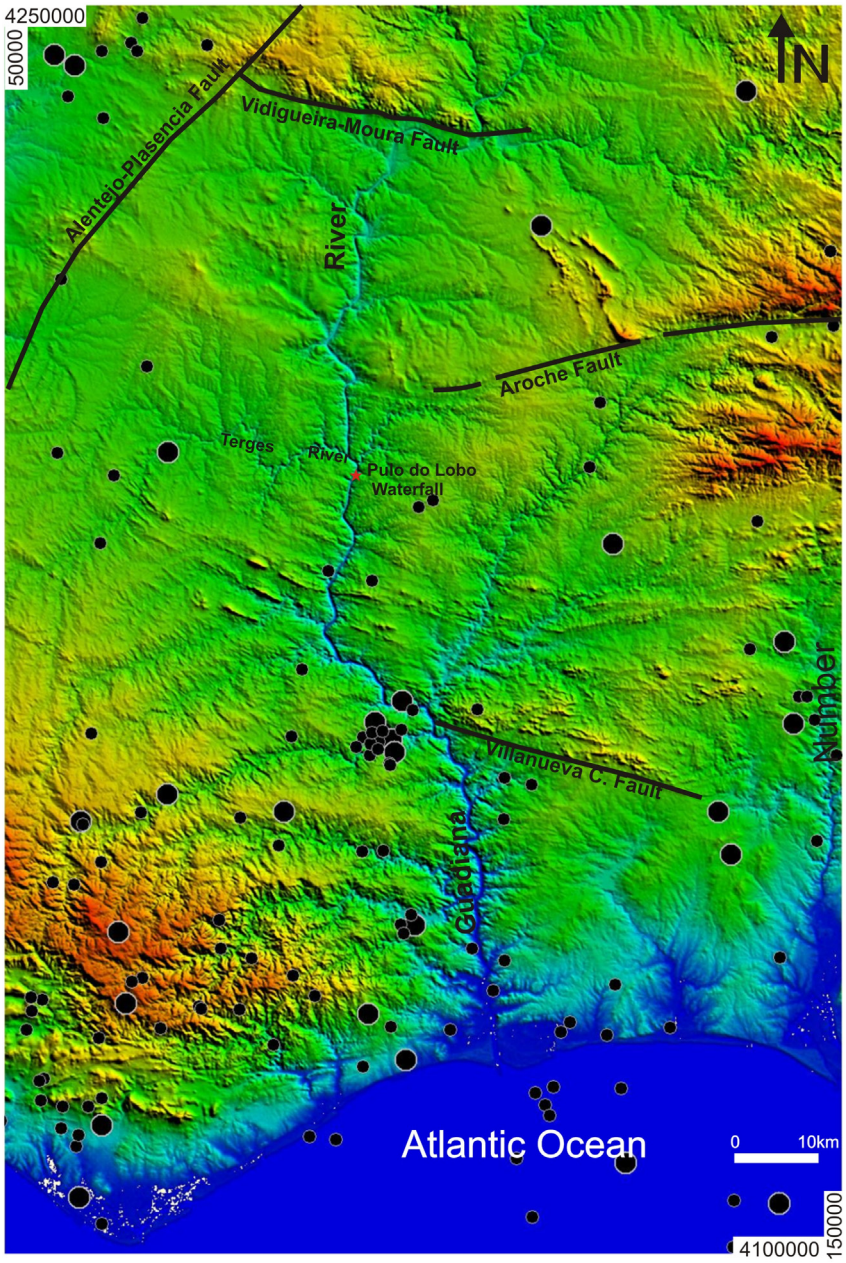


**Fig. 4.** Main Alpine faults and earthquakes of the study area and surroundings. Seismicity is scarce and concentrates mainly near the coast and Guadiana River mouth. Data filtered from the catalogue provided by the Instituto Geográfico Nacional de España (ww.ign.es). Small black dots display magnitudes 2–3 and great black dots display magnitudes 3–4 (www.ign.es; UTM Coordinates in meters. Zone 30).

approximately coincides with the reach in which the river acquires an estuarine nature and the ST finally disappears. The estuarine reach of the Guadiana gorge widens close to the river mouth when it cuts through the Pliocene deposits. It features a mesotidal regimen and tidal influence penetrates >50 km inland to Mértola. The estuary depth ranges from 5 to 17 m (Morales, 1997), but inland the channel becomes entrenched up to some 80 m under the mean sea level (Wolanski et al., 2006). A ~20 m-thick prodeltaic wedge occurs at the estuary mouth and this structure has been related to the last transgression stage, when a sea-level rise flooded the estuarine valley (Lobo et al., 2001, 2003; Boski et al., 2002). The lack of substantial deltaic deposits at the Guadiana River mouth, contrasting with the situation of its neighboring Guadalquivir River in which a large prodelta is found despite its shorter length, may be attributed to its lower discharge of 80 $m^3\ s^{-1}$ versus 160 $m^3\ s^{-1}$ for the Guadalquivir. This scarcity of discharge of the Guadiana basin, attributable to its development on the impervious Variscan rocks along with a lack of high headwater relief, may be important for understanding the erosional character of the canyon and its flooding behavior.

## 3. Materials and methods

To characterize the factors contributing to the formation of the ST of the Guadiana River, we compiled information about joints and faults, rock hardness, mean and maximum flood discharge recorded during the last 3000 yr, post-Miocene sea level curves, and cosmogenic data from the ST.

Based on geomorphological criteria, we selected three sites to collect structural and lithological hardness data (Fig. 7): (1) the Pulo do Lobo fall, whose knickpoint represents the main break-in-slope, incising an inner channel that develops the ST, (2) the Terges site upstream from Pulo do Lobo, the start of the well developed ST but still acting as a

**Fig. 5.** ST along the studied area. (A) Strath surface at the Terges River confluence during the ordinary water stage and (B) in 2012 during a low magnitude flood. (C) Incised ST at Pulo do Lobo area during ordinary water stage. (D) The incised ST can also be seen in the 1997 medium-high magnitude flood. (E) Pulo do Lobo waterfall and potholes. (F) ST dissected by the inner channel. (E) ST in patches at Mértola town during 2012 flood.

floodplain, showing rapids and a small inner channel and, (3) the Rocha da Gale site farther downstream with an open ST and small rapids.

The structural data obtained were focused mainly on joint and fracture orientation analysis and relationships with the drainage network. We measured joint orientations to explore the possible relationship between river pattern and ST development with a set of joints. We analyzed this at the three sites described above and compared these results with the orientations of straight river segments derived from a 25 m resolution DTM. Digital elevation data were obtained from the Shuttle Radar Topography Mission (SRTM) 1 Arc-Second Global (Spatial Resolution 30 m). ArcGIS Spatial Analysis and Spatial Statistics tools were used to measure the direction of straight river segments. We chose segment lengths between 200 m and 2000 m to analyze linear valley orientations and measured a total of 288 segments.

Given that rock erodability must be taken into account for waterfall development, we obtained surface hardness values (Schmidt hammer rebound test - HR) in outcrops using a Schmidt hammer. Rock hardness analysis was conducted at two working scales. First, hardness measurements were obtained throughout the study area (Fig. 7), differentiating between reaches upstream (Fig. 7A) and downstream from the Pulo do Lobo fall (Fig. 7B). Then, in a more detailed study (Fig. 7A1), we collected samples regularly every 50 m along a transect in the Pulo do Lobo knickpoint zone. We acquired more than the number of measurements suggested by Selby (1980) and measured at least 30 rebound values per site as recommend by Niedzielski et al. (2009). To avoid disturbances in HR results due to weathering, we took all the samples under the same meteorological conditions at a short distance to the river channel. Schmidt hammer readings were obtained in a transect from the banks to the river channel as shown in Fig. 7.

We obtained sea level curves from other studies (Haq et al., 1987; Shackelton, 1987; Boski et al., 2002; Lobo et al., 2003).

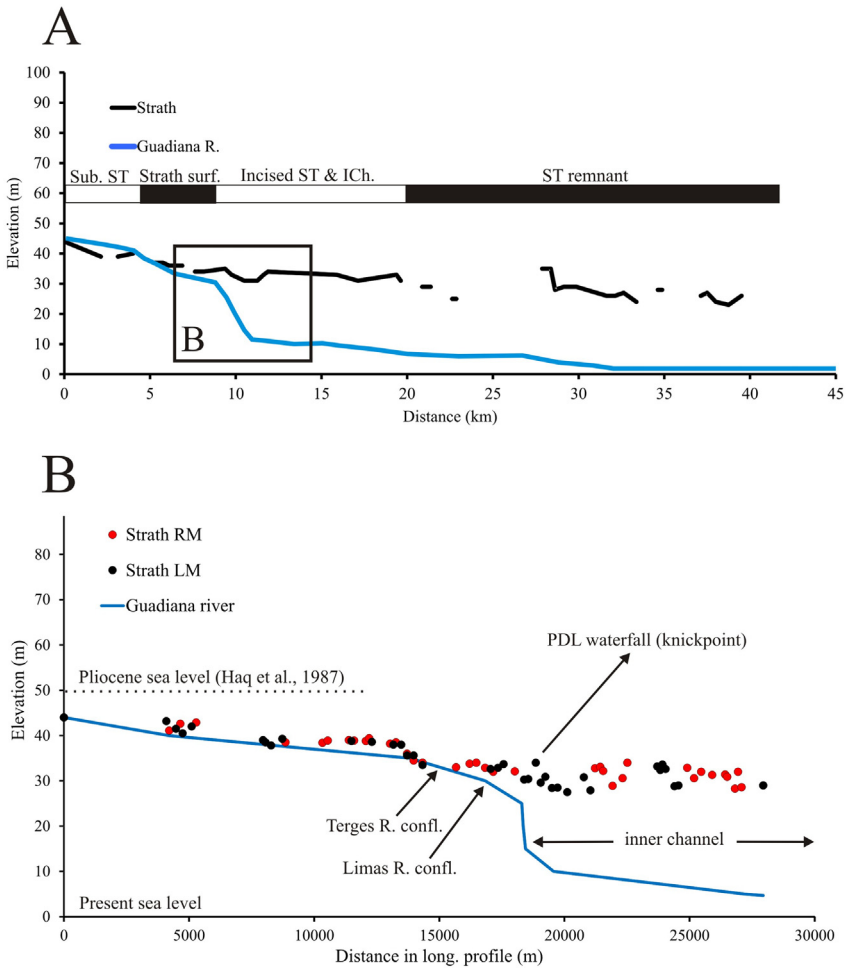


**Fig. 6.** Longitudinal profile of: (A) ST on the entire area, from Mosteiro to downstream Mértola, showing the four strath stages (submerged strath, flood-prone strath, incised ST and patched ST). (B) Detailed longitudinal profile in Pulo do Lobo area, showing height locations on ST in right (red) and left (black) margin. The dashed line indicates the approximate sea level position from the Pliocene (Haq et al., 1987) to the present. (For interpretation of the references to colour in this figure legend, the reader is referred to the web version of this article.)

Recent discharges and palaeofloods were taken from previous studies (Ortega, 2007; Ortega and Garzón, 2009) by means of slackwater deposits over the banks higher than the ST. The palaeoflood record runs up to 3000 BP cal. yr. We were not able to estimate older discharges due to the lack of previous fluvial deposits such as boulders or terraces in the studied area.

The ST and knickpoint lip were dated by cosmogenic nuclide ($^{10}$Be). We used cosmogenic analysis to determine the age of ST exposure. Additionally we used cosmogenic ages at different channel incision levels of the ST to obtain a relative incision rate by subtracting the average age between two levels. We sampled different sections on quartz lenses contained within schists, selecting distinct sites along the ST upstream and downstream the present active knickpoint (Fig. 7): bedrock forming the ST in the Pulo do Lobo area downstream from the knickpoint on the left margin (group A in Fig. 7), bedrock forming ST with potholes around the knickpoint lip considered a more active area (group B in Fig. 7) and bedrock at the ST upstream from the knickpoint on the right margin (group C in Fig. 7). Samples were chemically processed using standard procedures and surface exposure ages were calculated using the CRONUS-Earth calculator v2.2. Measurements of $^{10}$Be/$^{9}$Be were made at the Center for Accelerator Mass Spectrometry of the Lawrence Livermore National Laboratory (LLNL).

**Table 1**
Discharges and related unit stream power, velocity and water depth (after Ortega and Garzón, 2009).

| Discharge | Unit stream power ($W \cdot m^{-2}$) | Velocity ($m \cdot s^{-1}$) | Water depth (m) |
|---|---|---|---|
| Maximum recorded flood (e.g.:1603 CE, 11,000 $m^3 \cdot s^{-1}$) | 220 | 5–14 | 7–19 |
| Medium magnitude flood (e.g.: 1997 CE, 7000 $m^3 \cdot s^{-1}$) | 155 | 4–12 | 4–16 |
| Low magnitude flood (e.g.: 1996 CE, 2500 $m^3 \cdot s^{-1}$) | 13 | 3–8.6 | 4–12 |

## 4. Results

### 4.1. Lithological control on the drainage pattern and ST: Rock hardness analysis

The rock hardness analysis enabled us to examine rock factors like lithology and fracturation and other morphologies existing along the reach, such as rapids or waterfalls.

Most of the ST developed on phyllites of the Pulo do Lobo formation (see Fig. 3). Overall, these deposits offer low HR values of around 20–30 (Fig. 8). As suggested by Hancock and Anderson (2002), such values indicate that rocky outcrops are relatively erodible, both laterally in periods of stability and vertically during times of incision. This great homogeneity of the formation determines that it is an ideal setting for the development of a vast ST. However, despite this apparent homogeneity of materials, in the knickpoint Pulo do Lobo region, the phyllite formation shows many quartz veins running normal and parallel to

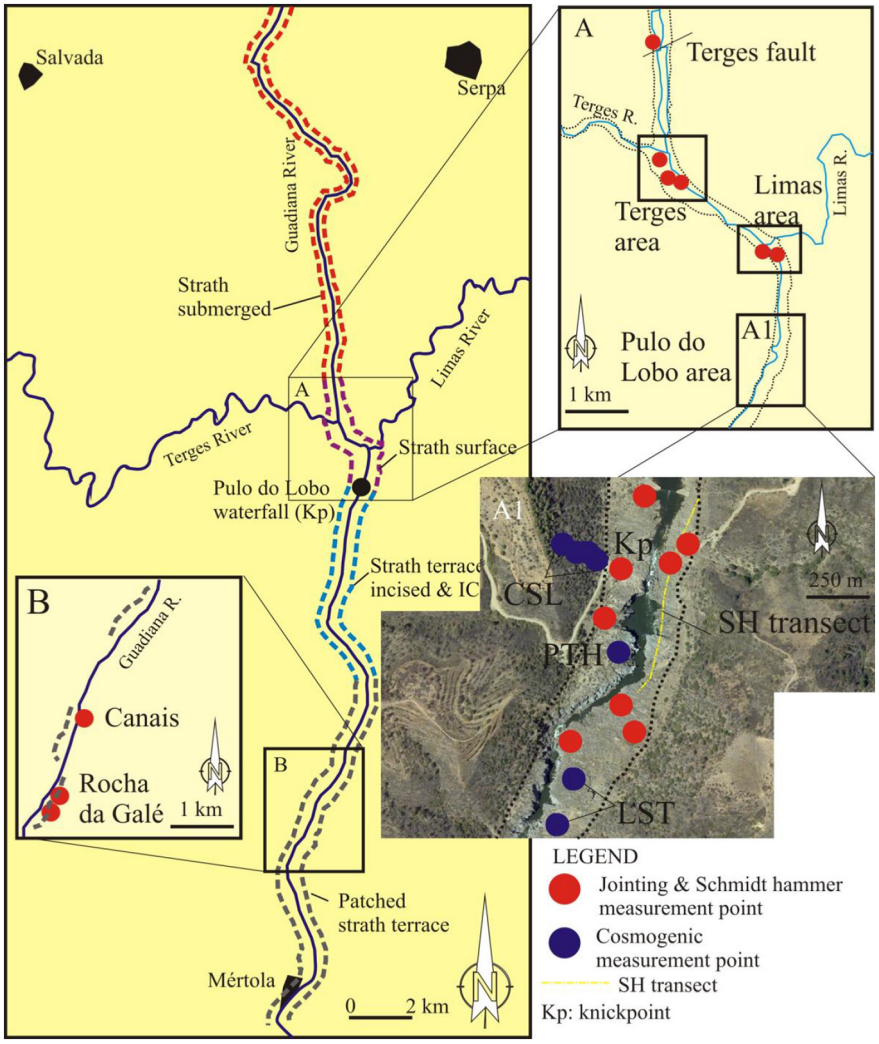


**Fig. 7.** Map of the studied area with the main surveyed reaches. (A) Three sub-reaches north of the Pulo do Lobo area. (A1) The main studied zone of Pulo do Lobo waterfall and start of incised ST. (B) Reaches south Pulo do Lobo. Different strath levels are classified as: submerged strath in the red dashed line, flood prone strath in the purple dashed line, incised ST in the blue dashed line, ST in patches in the grey dashed line. Blue circles indicate cosmogenic measurements, red circles joint and Schmidt hammer measurements, yellow dashed line Schmidt hammer transect. (For interpretation of the references to colour in this figure legend, the reader is referred to the web version of this article.)

the main river direction associated with fold hinges. The quartz veins also show high local variation on the meter scale, which conditions their HR values. Thus, subtle differences could be related to rock type such that the mean HR = 30 for schist, and this value increases to HR = 37–46 if the proportion of quartz veins increases in the schists (at the Pulo do Lobo fall and other areas). The main lithological change, however, occurs in the lower canyon reach at Rocha da Galé, where higher values (HR = 50–60) were recorded due to the presence of quartzites and dacites.

In morphological terms, results indicate (Fig. 8) a general trend towards higher HR values (45–50) in zones of rapids or knickpoints, and medium values (24–30) in the remaining zones where the ST is well-formed. Hammer rebound values fluctuate throughout the study area depending on vein quartz contents closely related to metric anticlinal folds. Small rapids near the Limas River's confluence returned higher HR values (two rapids: LR-1 HR = 44.5 and LR-2 HR = 44.9). Downstream from the knickpoint, we observed similar values (HR = 53.3) for another rapid (sample PL-T1–12). However, other areas of rapids show lower mean HRs than expected (HR = 19.7–32.7 for TR-1 and HR = 32.6 for CN-1). Additional exceptions showing low values (HR = 15–26) are attributed to local tectonic discontinuities. Nevertheless, these structural elements seem to be older than the ST as this does not appear displaced.

In spite of its flat configuration, the ST shows a rough morphology at the metric scale due to the local increase in quartz veins interbedded in the schists of the Pulo do Lobo Formation. Hence, due to the increase in bedrock hardness, the best configuration to reduce the longitudinal profile of the river is the concentration of water flow in an inner channel, as occurs downstream Pulo do Lobo fall. In effect, the Guadiana River is currently lowering its profile by means of headward erosion (Garzón et al., 2008). However, although locally the fall does show a greater hardness, this only represents a slight local anomaly within a recurrent lithology, which on its own does not explain the large jump it creates. We should therefore consider that the fall represents a temporal obstacle in the progressive downcutting of the lower Guadiana reach.

### 4.2. Drainage pattern and structural control

To understand the role of structure in ST formation, we examined the drainage pattern and then correlated this pattern with the fold axes and the directions of the main families of fractures. A priori, all these factors could have played an important role in the development of the Guadiana River's ST, as occurs elsewhere (Pratt et al., 2002; Wegmann and Pazzaglia, 2002).

The drainage network of the final Guadiana reach reveals a deep, densely dissected landscape showing a complex angular pattern with

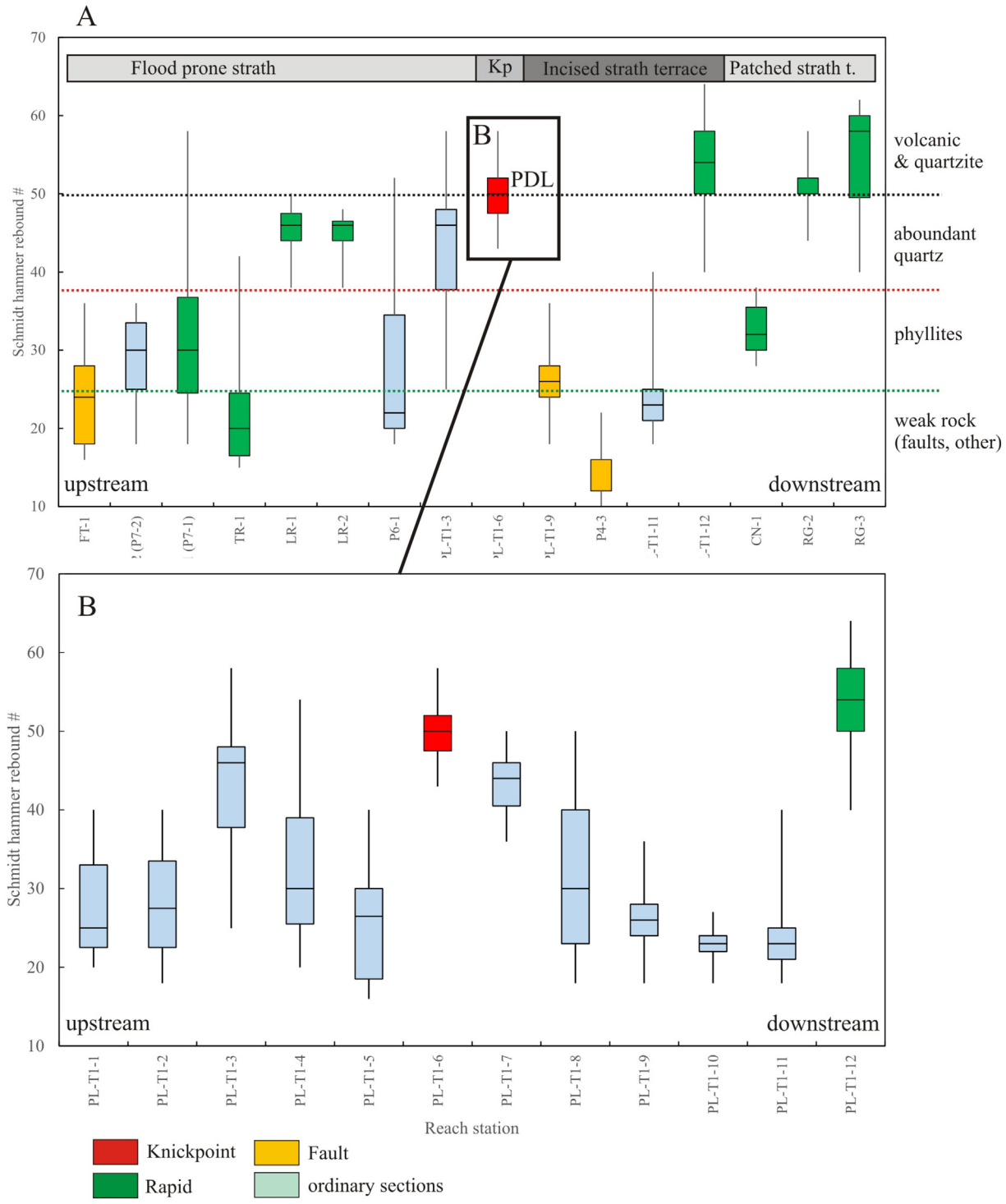


**Fig. 8.** Schmidt hammer values obtained in the studied reaches. Knickpoint: red, rapids: green, yellow: fault and fracture areas, blue: ordinary sections. (A) Schmidt hammer rebound number (HR) for the whole area upstream and downstream PDL knickpoint (Kp) related to different lithologies and morphologies. (B) Pulo do Lobo detailed transect along the ST upstream and downstream of the knickpoint. (For interpretation of the references to colour in this figure legend, the reader is referred to the web version of this article.)

entrenched and contorted meanders (Fig. 9). The valley's drainage divides define a narrow level of regional flattening (~160 m high) resulting from degradation of the upper planation surface. This embedded surface marks a descending trend consistent with that of the Guadiana River, indicating a stage of development prior to generalized fluvial entrenchment. This underlines the complexity of the current drainage network that can be interpreted as the result of superimposition over the preexisting Cenozoic sediments, whose remnants are still preserved on the planation surface. The geomorphic evolution described above could explain the contrast between the linear straight slope profile of the Guadiana's canyon compared to the high sinuosity of its incised tributary streams, which have suffered a long process of integration towards the Guadiana River.

Within this intricately dissected landscape, the Guadiana River takes on a net N—S direction resulting from the north trending longer reaches displaced by shorter transverse reaches tracking NE-SW and NW-SE.

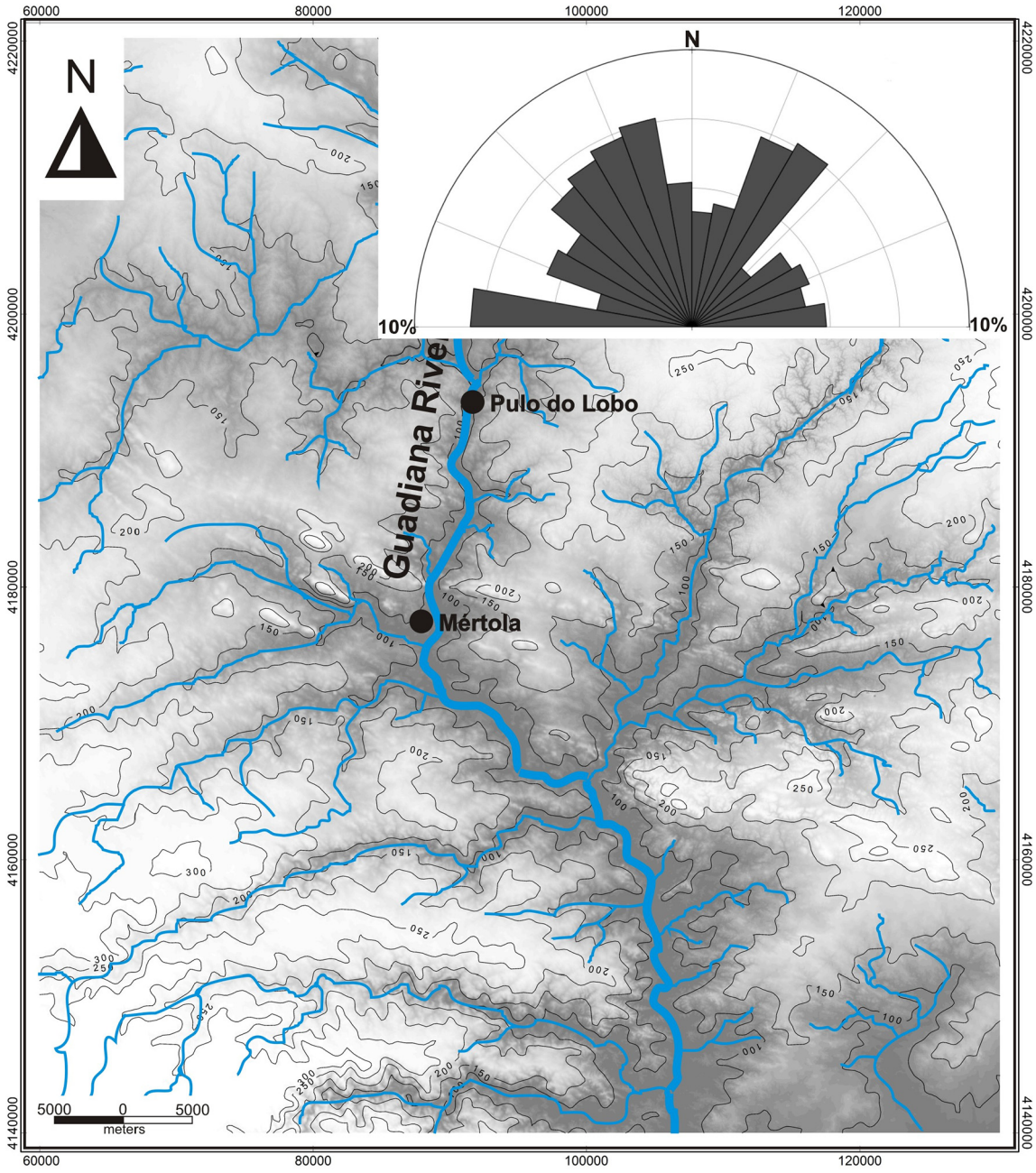


**Fig. 9.** Drainage pattern of the study and surroundings areas (UTM Coordinates. 60 Huso 30). Orientations of river segments are displayed in the rose diagram (n = 288 data). Directions of E-61 W, NW-SE and NE-SW dominate. The Guadiana River exhibits a dominantly N—S 62 path, not very remarkable in the rose diagram. (For interpretation of the references to colour in this figure legend, the reader is referred to the web version of this article.)

Our river segment orientation analysis reveals wide variation in trends dominated by orientations of ~N35°, N95° and N340° (Fig. 9). Orientation directions of NW to WNW coincide with mapped Variscan structures. Fig. 10A shows mesoscopic fold axes and foliation planes measured near the Pulo do Lobo fall. The structures there exhibit a N100° main trend coincident with some tributary segments (Fig. 10B).

On the other hand, according to our joint orientation analysis, N—S to NE-SW orientations prevail with a less represented E-W family (Fig. 10C). N—S joints are the most pervasive along some segments of the Guadiana canyon. They show metric spacing and a significant length of several of tens of meters, following the Guadiana valley and controlling the canyon's direction (Fig. 10D). N—S segments are mainly associated with longer valley segments. Further, their statistical representation was smaller than the shortest dominant segments in the tributaries. NE-SW fractures appear as responsible for the NE river segments. These results reflect the important role played by inherited structure in the drainage network pattern.

The intersection of N—S and NE-SW families gives a broken appearance to the inner channel edges and promotes the formation of blocks that drop within the inner channel, along or at the foot of the slopes. In some cases, rapids appear to be related to N100° upright folds developed on hard rocks. This could be linked to the predominant mode of bedrock erosion: quarrying, plucking and clast wedging (Hancock et al., 1998; Whipple et al., 2000) as is also shown in Anton et al. (2015) where the existence of several joint sets and the orthogonal pattern plays a key role in block removal and gorge formation.

We found no clear evidence of ST displacement due to faulting. As shown in Fig. 6, the difference in elevation is significant for the inner

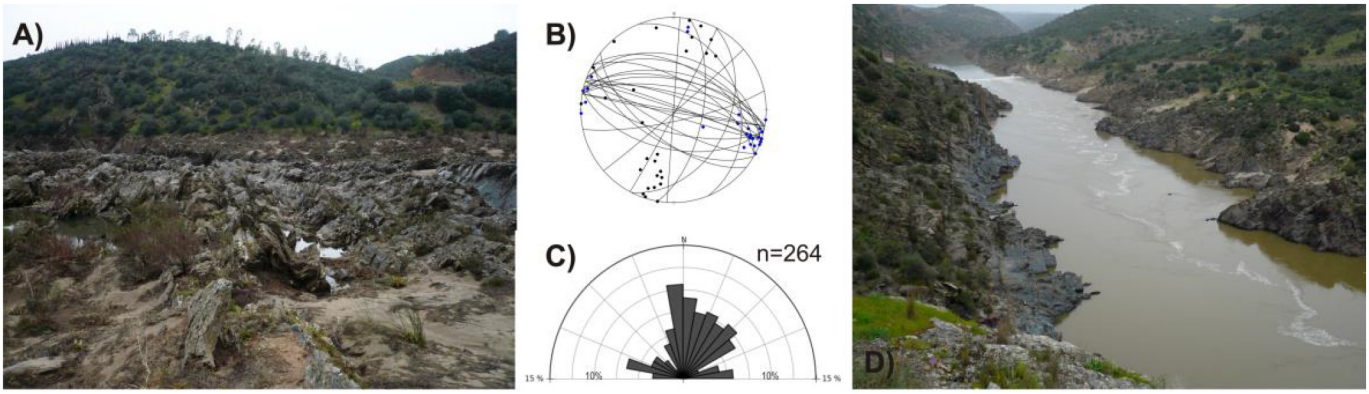


**Fig. 10.** (A) N100° metric and decametric upright folds in the ST. (B) Stereographic projection of foliations and fold axes on the study sites. A WNW trend dominates similar to Variscan regional structure directions. Foliation indicated by great circles and poles (black points); Fold axes indicated by blue points. (C) Guadiana River canyon parallel to N–S joints close to the Pulo do Lobo waterfall. At a regional scale, N–S fractures are pervasive with metric spacing. (D) The rose diagram shows that joints trend N–S to NE-SW with a mean direction of 10.2°. Also a roughly E-W direction is present. We measured 264 joints at the Terges, Pulo do Lobo and Rocha Gale sites. (For interpretation of the references to colour in this figure legend, the reader is referred to the web version of this article.)

channel at Pulo do Lobo but not for the ST. Some very small scarps, <2 m high, can be attributed to relief roughness. Although we cannot rule out the tectonic control of the drainage network, we detected no evidence in the Guadiana valley of local structures formed during post-Alpine tectonic activity that could be responsible for the development of the ST.

### *4.3. Climate controls on the Guadiana ST: Sea level changes and cosmogenic dating of surface exposure*

Owing to its close proximity to the mouth of the Guadiana, the Pulo do Lobo area has been constantly affected by sea level changes, at least from the lower Miocene to the present and especially during the marked sea level changes of the Quaternary. These changes induce periods of aggradation during sea level rises and outwash of deposits when sea levels drop. However, as mentioned by Merritts et al. (1994), there could be a mismatch such that the age of original valley incision does not correspond to the age of final abandonment of strath surfaces.

Sequences of sea level rises and falls may fill or wash sediments downstream, thus exposing surfaces of bedrock reaches. Interactions between cosmic rays and elements in a rock produce cosmogenic isotopes. Thus, cosmogenic nuclides in samples from the Pulo do Lobo ST may be interpreted as corresponding to times of rock surface exposure following the retreat of cover sediments and water, leaving the outcropping rock surface free to receive cosmic rays.

In the Pulo do Lobo fall zone, cosmogenic ($^{10}$Be) dating was performed for the points shown in Fig. 7 (Garzón et al., 2016). These figures offer information on the evolution of the ST if we consider that cosmic rays will start to impinge on the ST surface once it is clean of sediments. Results may be subject to local topographic variations. For example, zones of harder rocks such as those with roughness conferred by quartz veins will generate elevated zones in the ST itself and these will be cleared of sediment cover earlier because they are higher. The results of our cosmogenic exposure analysis are provided in Table 2.

The three zones where the cosmogenic dating was performed are: (1) The left ST (LST), lying +27–35 m a.s.l. and dated at 35–69 kyr. (2) The potholed ST (PTH) close to the knickpoint and covered with giant potholes, which is the most active zone of the ST occurring at +17–20 m a.s.l. and dated at 16–20 kyr; (3) The canyon slope (CSL), at an altitude of +42–62 m a.s.l. where the entrenchment was dated at 21–30 kyr. Dates were fairly irregular and inconsistent with their altitudes (see Table 2) as they were low with respect to the PTH, which is a lower and more active zone.

Although not one of the main objectives of this study, we can establish relative incision rates based on the average cosmogenic ages of each level analyzed. To summarize these results, if we consider the extreme data obtained in the left ST (LST), that is, maximum and minimum

**Table 2**
Cosmogenic nuclide dating of the samples analyzed clustered into three groups: LST = ST – left margin downstream from KP; CSL = slope – right margin of canyon valley; PTH = knickpoint lip – potholed ST.

| | Sample ID | Latitude (degree) | Altitude (m a.s.l.) | Thickness | Shielding | NBe[a] | Be age (ka)[b] |
|---|---|---|---|---|---|---|---|
| Strath terrace (LST) | PL10-1 | 37.80 | 34.94 | 0.97 | 0.99 | 0.16169 ± 0.00870 | 38.22 ± 4.14 (2.06) |
| | PL10-2 | 37.80 | 34 | 0.97 | 0.91 | 0.18202 ± 0.00620 | 46.71 ± 4.65(1.59) |
| | PL10-3 | 37.80 | 35 | 0.96 | 0.94 | 0.25301 ± 0.00880 | 63.91 ± 6.34(2.22) |
| | PL10-4 | 37.80 | 35 | 0.98 | 0.94 | 0.28168 ± 0.01050 | 69.85 ± 7.00(2.60) |
| | PL10-5 | 37.80 | 32.4 | 0.98 | 0.94 | 0.16117 ± 0.00610 | 39.75 ± 4.02(1.50) |
| | PL10-6 | 37.80 | 29.72 | 0.98 | 0.99 | 0.17931 ± 0.00650 | 42.06 ± 4.21(1.52) |
| | PL10-7 | 37.80 | 28 | 0.97 | 0.99 | 0.14856 ± 0.00590 | 35.06 ± 3.57(1.39) |
| | PL10-8 | 37.80 | 27 | 0.99 | 0.95 | 0.15982 ± 0.00580 | 38.86 ± 3.91(1.41) |
| Slope (CSL) | PLS10-4 | 37.81 | 43.81 | 0.98 | 0.91 | 0.09872 ± 0.00440 | 24.84 ± 2.60(1.11) |
| | PLS10-5 | 37.81 | 47.46 | 0.96 | 0.89 | 0.08152 ± 0.00390 | 21.38 ± 2.27(1.02) |
| | PLS10-8 | 37.81 | 52.91 | 0.98 | 0.87 | 0.11603 ± 0.00510 | 30.59 ± 3.19(1.34) |
| | PLS10-10 | 37.81 | 62.89 | 0.99 | 0.87 | 0.10237 ± 0.00490 | 26.55 ± 2.82(1.27) |
| Knickpoint (PTH) | PLRB10-1 | 37.80 | 20.09 | 0.96 | 0.99 | 0.07798 ± 0.00350 | 18.62 ± 1.94(0.84) |
| | PLRB10-2 | 37.80 | 17.73 | 0.98 | 0.99 | 0.06891 ± 0.00410 | 16.20 ± 1.82(0.96) |
| | PLRB10-4 | 37.80 | 17.58 | 0.97 | 0.99 | 0.08549 ± 0.00380 | 20.13 ± 2.10(0.90) |

[a] NBe are corrected concentrations of atoms, unit: 106 atoms/g. Be.
[b] Ages given in ka with analytical errors in brackets

ages of 69.85 ± 7 kyr and 35.06 ± 3.57 kyr and maximum and minimum heights of +35 m and + 27 m, we obtain a mean relative incision rate for this zone of 0.022 cm $yr^{-1}$. In contrast, to calculate the relative incision rate in the more active zone of the knickpoint (PTH), maximum and minimum ages of 20.13 + 2.10 and 16.20 + 1.82 kyr and heights of +20 and +17 m were used to give a relative incision rate of 0.06 cm $yr^{-1}$. This rate is greater than the mean value obtained in the left ST zone (LST) and may be explained by greater erosional activity in the ST zone close to the channel linked to knickpoint migration. However, it should be noted that this last result was based on a lower time interval and fewer dated samples. To compare these results in context, if we consider an entrenchment of some 15 m of the Pulo do Lobo waterfall over ~20 kyr, this gives an incision rate of around 0.075 cm $yr^{-1}$, which is somewhat higher than our rate (but of the same order of magnitude). These estimates can only be taken as ranges of relative incision. In contrast, the slope data (CSL) are not so well related to their respective heights. Estimated ages were more recent than for the ST and similar to those obtained for the PTH group, despite their higher altitude. We interpreted these as reflecting slope activity more than incision of the river Guadiana, although this could imply a complex incision in space and time.

Cosmogenic data are illustrated together with the eustatic sea level curve for the Guadiana estuary. In Fig. 11, sea level changes are summarized alongside the periods of fluvial deposition in the estuary proposed by Boski et al. (2002) based on the works of many authors. Thus, Haq et al. (1987) and Shackelton (1987) reported sea level rises of up to +150 m over the current level for the early and middle Miocene and Pliocene, along with falls of up to −50 m in the late Miocene and also of −120 m during the Quaternary. Boski et al. (2002) and Lobo et al. (2003) assumed values of this order for the Gulf of Cádiz. In borehole surveys at the mouth of the Guadiana, a base level of deposits of fluvial origin associated with isotope stages 5 and 3 has been detected (Boski et al., 2002).

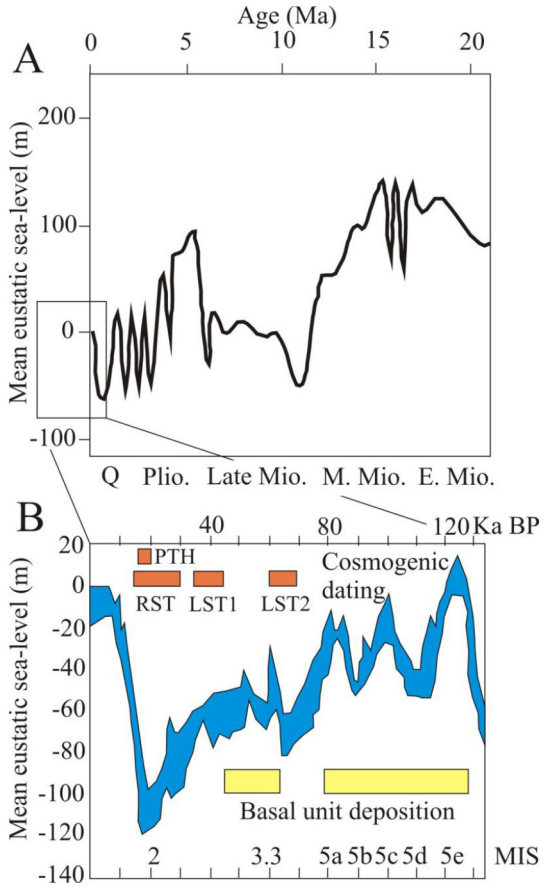


**Fig. 11.** Sea level oscillations during Miocene-Quaternary according to Haq et al. (1987); Shackelton (1987); Boski et al. (2002) and Lobo et al. (2003). (A) Eustatic changes during last 20 Myr. (B) Recent sea levels in the last 120 kyr with periods of fluvial activity and estuarine deposition at Guadiana River mouth (basal unit deposition, Boski et al., 2002 and Lobo et al., 2003) and cosmogenic dating at Pulo do Lobo ST.

## 5. Discussion

Our study considers three determining factors for the genesis and evolution of a ST: (i) lithology, (ii) tectonic structures and (iii) sea level changes.

### 5.1. Lithology

Through rock hardness analysis, we established the clear control of the Pulo do Lobo Formation in the development of the ST. The monotone series of lithologies repeated along almost 20 km provides the ideal conditions for the formation of such a large and regular surface. The greater presence of quartz accumulations locally increases rock hardness and this generates changes in ST roughness and metric scale ridges. However, the ST does not only appear on this formation but continues downstream on some volcanic Carboniferous rocks and also in quartzite outcrops, although it is more poorly developed over these units. In summary, although lithology emerged here as an influential factor, the extension of the ST across multiple lithologies indicates that lithology was not the primary control on strath configuration. However, we could argue that rock characteristics were responsible for the evolution of the terrace, delaying or expediting inner channel migration according to local rock hardness, and potentially favoring lateral bedrock erosion in weaker rocks according to the work of Stokes et al. (2017).

### 5.2. Tectonic structures

Our structural analysis revealed the impact of tectonic structures on the geometry of the drainage pattern and their active contribution to its erosion. However, we found no evidence of compartmentalization in blocks bounded by faults and related scarps, which would have displaced the ST and controlled its formation (e.g., Pratt et al., 2002; Wegmann and Pazzaglia, 2002). Although seismic activity was considerable in the submerged zone of the Gulf of Cádiz (Custódio et al., 2015) and GPS data point to recent tectonic activity in SW Iberia (Cabral et al., 2017), this activity was restricted to marine and coastal areas, diminishing towards the emerged domain and practically disappearing in the vast basement outcrops (Fig. 4). The ST surface in the study area has a homogeneous nature and has developed consistently with the canyon width, with its margins parallel to the valley slopes. Notwithstanding, the configuration of the ST in this zone is paired, whereas observations by Bull (1990) and Personius et al. (1993) indicate that STs in tectonically active zones are usually unpaired. The great homogeneity of ST heights on both sides of the inner channel does not allow us to infer asymmetries produced by tectonic structures.

### 5.3. Sea level changes

In alluvial fill terraces, the age of the terrace surface does not necessarily correspond to the age of the deposit over which it developed (Leopold and Miller, 1954). Determining the origin of STs is even more complex. If they have an alluvial cover, the age of the alluvium may not match that of the strath, and if they lack deposits, they could be older surfaces exhumed from beneath a sedimentary cover. Further, this exhumation may be slow and progressive as it represents the gradual exposure of a flat fluvial bed shaped by the river. The formation of a ST as large and regular as that described for the Guadiana River would

require a long period of stability because the rigid margins of bedrock rivers imply a slow response to base level changes (Shepherd and Schumm, 1974).

In the only detailed study known about lower Guadiana terraces, Feio (1946) correlated the ST development to the Riss cold period. This author adopted the established correlation model relating the altitudinal levels of the lower Guadiana River with glacial regressive stages. In the absence of further data, he considered that the abrupt incision of the current valley downstream of Pulo do Lobo had eroded during the Würm stage, implying that the ST above had to correspond to the Riss stage. He considered, however, that the genesis of such an extensive ST would require a prolonged regression to develop. To justify its homogeneous morphology without being degraded afterwards due to the Würm regression, Feio suggested that a pre-Würm transgression should have covered the ST with deposits. As a consequence, the ST had to be considered an exhumed Riss surface.

Taking into account the current state of knowledge of Quaternary marine highstands, the sea is only assumed to have reached higher elevations to the present during the Eemian (MIS 5e, Fig. 11). On the Algarve coast, it would be between 3 and 5 m higher (e.g., Pais et al., 2012). It is therefore difficult to accept that this transgression affected a ST that reaches a 40 m height, unless significant uplift occurred, yet there is no evidence of significant observed faults in the ST.

The idea suggested by Feio (1946) that the ST represents an exhumed surface is consistent with the context we described upstream of the Pulo do Lobo fall. We should highlight the context of the canyon upstream of the Pulo do Lobo fall, where the strath still constitutes the present bed of the Guadiana and gradually crops out from the water surface as the channel concentrates in a deep, narrow course. Within this geological framework and considering a preexisting ST, cosmogenic $^{10}$Be dating from the Pulo do Lobo waterfall (rather than the time of ST formation) would indicate the evacuation of the sedimentary cover and retreat of the knickpoint due to Quaternary sea level fall. This could also be coupled with climate related changes with effects on hydrological variables such as river discharge. The low sea levels persisting in the Pleistocene with average depths of −60 m can explain the incision of the inner ST channel within the old valley bottom and its entrenchment through a very active headward retreat. Cosmogenic nuclide dates might be more or less coeval with the time when the river became incised and abandoned its former bed at the specific dated area. Cosmogenic data indicate ages starting at 69.85+ 7 kyr.

The higher Eemian sea level stage represents a warm climate and increased soil formation and weathering that would have reached areas close to the Pulo do Lobo waterfall. The subsequent Würm recession would drive new erosion at the base of the knickpoint, and the consequent aggradation could occur in coastal areas within an expected delay. In spite of the general lack of deposition at the Guadiana mouth, a small prodelta occurs showing 50 kyr old basal gravels (Lobo et al., 2003). The comparable nature between both dates allows us to relate the load increase with erosive reactivation at the KP and the cosmogenic age of dismantling the ST sedimentary cover.

Given the elevation at which the ST of the Pulo do Lobo developed (at least 40 m a.s.l.), we may rule out its formation during the sea level fluctuations of the Quaternary (see Fig. 11). Furthermore, there is no evidence of stepped surface erosion accompanied by substantial tectonic elevation during this period.

Further significant support for the pre-Quaternary age of the ST within the context of an uplifted area can be found in the longitudinal profile analysis of the tributaries of the lower Guadiana River conducted by Garzón et al. (2008). The tributary streams of the upper reach (Terges and Limas rivers) show a concave, well-adjusted profile with the base level on the strath. In contrast, the situation changes radically below the knickpoint, and incoming streams show significant convex profiles marked by the sharp gradient increase in their lower reach interpreted as the result of greater subsidence activity in the Guadiana mouth. The concave, more mature profile of the tributaries upstream contrasts with those of the lower reaches, which are adapted to the new base level originated by the Guadiana channel once it entrenched in the ST. This implies that the strath represented the base level of the upstream rivers and of their entrenched drainage network, and that suggests a long time for adjustment.

The significance of the Pliocene transgression followed by the abrupt Quaternary incision might be a key to understanding river evolution in the area. The Pliocene transgression sea level was around 50 m higher than at present (Pais et al., 2012). During this period the deposition of shallow platform and deltaic sediments culminated with a significant fluvial aggradation stage (Leyva and Ramírez, 1983). Alluvial fans and braiding river deposits indicate high stream power and erosion and transport capacity (Salazar et al., 2016). In foothill areas, the deposits would reach higher altitudes, but this does not rule out that the main river valleys were still active, although aggradation could occur during sea higher stands.

The warm to subtropical climate of the early Pliocene (Lourens et al., 1996), along with a high and stable sea level (Miller et al., 2005), favoured weathering along with the larger load supply. This represents a favorable scenario to drive the widening of the canyon bottom, thus consolidating the large flat strath surface, which would be preserved thereafter under the last continental Pliocene sediments.

In Fig. 12 we provide a conceptual model of the evolution of the lower Guadiana with the Pliocene transgression covering a possible preexisting surface (stage I) and the start of sediment outwash and steady exhumation during the sea level drops of the Lower and Middle Pleistocene (stage II) and Upper Pleistocene (stage III). Finally, the last marine transgression during the Holocene again flooded the Guadiana estuary, with sea level maintained close to its current level (stage IV).

Throughout the Quaternary, deposits are scarce in front of the Guadiana mouth, but on the eastern side of the Guadiana River, the thick Pliocene unit appears dismantled and reworked in a stepwise fashion towards the coast (Leyva and Ramírez, 1983). According to Rodríguez-Vidal et al. (1993), another larger river flowed towards the Guadiana embayment in a SW direction. During the Pliocene regression, the configuration of the watercourse in the Cadiz Gulf was reorganized. The outlet of this palaeoriver was displaced southwards forced by the Guadalquivir basin's subsidence (Fig. 3B). Successive captures allowed the drainage network to dismantle the thick Pliocene sedimentary unit, reshaping its deposits in a terrace staircase towards the coast along successive Pleistocene oscillations.

This situation illustrates the different behavior shown by the Algarve and Guadalquivir morphotectonic domains. The absence of terrace remnants along the Guadiana canyon differs from the terrace staircases model (e.g., Bridgland and Westaway, 2008), which might be applicable, however, to the described Guadalquivir terrace system.

As a first approximation to incision rates, our value of 0.02 cm yr$^{-1}$ is somewhat higher than the suggested average rate of 0.015 cm yr$^{-1}$ for middle latitudes (Pitty, 1971), yet comparable to values reported for semiarid climate zones of 0.007 to 0.025 cm yr$^{-1}$ (e.g., Harden and Coleman, 1988). As in our case, many authors find temporal variations in incision rates (for example the 0.06 cm yr$^{-1}$ reported by Collins et al., 2016). However, these values are subsequent to the LGM, held responsible by other authors (Hancock and Anderson, 2002) for the increased incision rates. We could even speak of higher values if we consider the current total 15 m vertical drop of the inner channel in the ST for which rates of 0.075 cm yr$^{-1}$ could be estimated. Such values are consistent with the rates of 0.04 to 0.1 cm yr$^{-1}$ observed by others in knickpoint zones (e.g., Seidl et al., 1997). Much higher incision rates are often found, although they generally correspond to regions subjected to rapid uplift, unlike the present case (e.g., Wegmann and Pazzaglia, 2002). For a better understanding of incision rates, we would need to consider extending our sampling area to the upper strath zone and to the ST reaches in patches, since, as recognized by Whipple (2004), changes over time in river dynamics have been and are currently large.

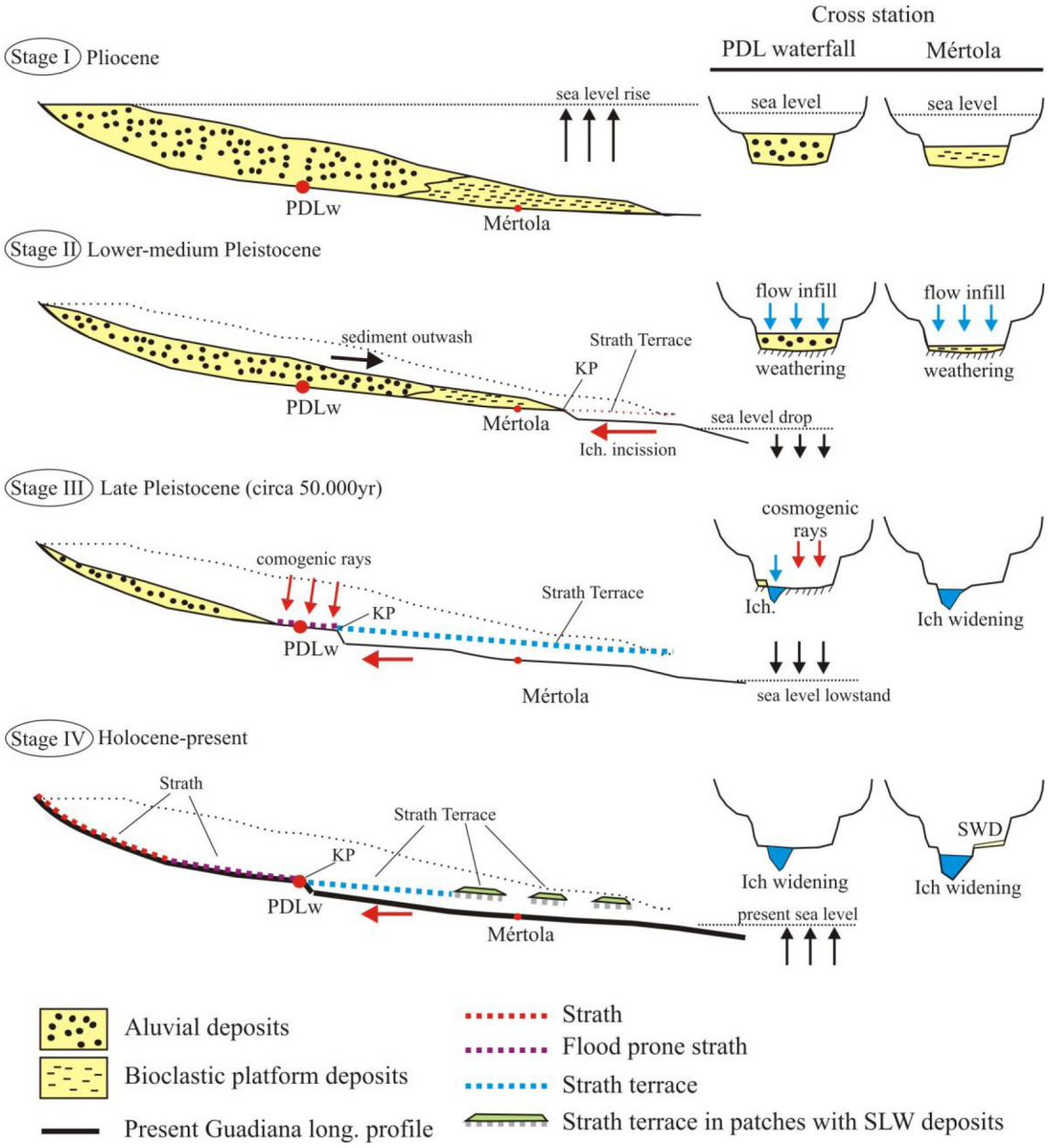


**Fig. 12.** Suggested evolution of lower Guadiana ST, from Pliocene till present. Stage I: fluvial deposition over the ST during Pliocene sea level rise. Stage II: sediment outwash and KP migration during Lower-medium Pleistocene sea level drop. Stage III: Knickpoint migration up to the present location of Pulo do Lobo waterfall (PDLw) and the start of cosmogenic radiation over the ST at Late Pleistocene. Stage IV: Inner channel widening and further erosion of the ST during the Holocene.

Sea level oscillations resulting from climate change have been proposed as one of the most effective mechanisms of ST generation, especially in periods of continental uplift (e.g., Pazzaglia and Gardner, 1993; Hancock and Anderson, 2002). The Pulo de Lobo ST would be more interpretable within the long-term period of slow of regional uplift on hard rocks and the coastal downwarping model described by Pazzaglia and Gardner (1993) during a stage of stability of sea level. Quaternary glacioeustatic level changes might not be responsible for the formation of the ST surface at the Guadiana canyon. This can be attributed to a much earlier event at least related to the Pliocene, involving the downwarping of the Guadalquivir depression at its boundary with the Iberian continental margin. The great extension of the ST and the lack of recent tectonic evidence in the Guadiana canyon make us consider it a relict morphology with a long genetic history.

In the genesis and development of the Pulo do Lobo ST there are two important factors to consider: the river's outflow in the subsidence zone coinciding with the flexure of the Guadalquivir Basin and the exceptional location of the Guadiana canyon. The Guadiana River setting at the boundary between the Algarve morphotectonic domains and the Guadalquivir depression implies a fringe area with different morphological responses. Despite the tectonic activity remaining in the submerged basin area, the continental zone behaves as tectonically stable blocks and its evolution would be controlled by the resistant Variscan substrate that defines local base levels. The current morphology that defines the mountain ranges and their bounding scarps are likely more associated with relict or exhumed differential erosion relief than with Quaternary or Late Cenozoic tectonics. The ST maintains its almost flat morphology with its much gentler slope than that of the modern Guadiana River within minor differential

controls of lithological origin but in the absence of evidence of recent tectonic deformation.

## 6. Conclusions

The lower Guadiana River features a ST carved in the metamorphic rocks of the Variscan basement. The ST is well preserved and covers a distance of 40 km in the canyon that characterizes the Guadiana valley along >140 km. In the strath, four areas of different characteristics and states of development can be distinguished: (1) the submerged ST or initial evolution stage; (2) the outcropping ST or active floodplain zone; (3) the incised and perched ST that is still prone to flooding when there are high magnitude floods; (d) ST levels appearing as patches that are gradually being eroded and so lose their longitudinal continuity. These levels represent a more advanced stage of evolution.

Although the formation of a ST is complex, our data serve to establish the factors that may have contributed to the formation and development of the strath examined here. According to existing regional approximations, the sea level changes that took place during the Quaternary cannot have played a role in the genesis of the ST. However, our cosmogenic element dating suggests an age for erosion of the sediment cover protecting the ST from cosmic rays rather than its time of origin. If we assume a long period of tectonic stability is needed for such a ST to develop, this should have occurred after the Alpine deformations at the end of the Miocene. Accordingly, the age indicated by our cosmogenic analysis would be related to the exhumation of a preexisting surface from the sedimentary cover.

For a strath to form within a bedrock channel, the prerequisites needed are changes in water discharge and sediment accompanied by temporal stability of the base level so that the valley bottom will widen sufficiently for it to develop a large flat surface. In the present case, the long period of tectonic stability of the zone positioned at a continental margin has determined the exceptional conservation and extension of the ST. Further development involved a subsequent intense process of incision controlled by the sea level drops during the Quaternary and subsidence in the Golfo de Cádiz to explain the entrenchment of the ST's inner channel. During this time interval, the ST has not been displaced nor destabilized, helping to preserve its regular morphology.

The preservation and development of this ST have been promoted by the hardness and homogeneity of its materials, especially in the Pulo do Lobo Formation. Further, the quartz veins present have exerted control on knickpoint migration and on stabilization in the zone of the Pulo do Lobo waterfall. Fracture geometry continues to play an important role in destroying the ST by favoring plucking erosion and influencing the ST's lateral extent via the orientation of joints perpendicular to the river.

Despite high unit stream power values and the intense erosive activity to which the knickpoint zone is subjected, the cosmogenic age range obtained within the transect of the waterfall zone is large and variable. Our results indicate a zone in a state of exhumation and/or retreat maintained over slow evolution. Dates for the higher samples of the ST indicate much older ages relative to the age of the knickpoint zone and its potholes, despite a continued incision process.

Results obtained highlight the gradual evolution from a flat riverbed to configure one regional extended ST outlining the transient stages of ST configuration. This context suggests that cosmogenic dates obtained at a ST may not represent its formation date, but rather the outcropping or exhumation date. Results reveal the prolonged persistence of the ST and the slow erosional activity at the KP. This slow evolution points out the restricted erosion in a river limited by a shortage of sediment load despite high stream power expenditure during large flash floods.

The present study represents an attempt to envisage past geomorphological stages to understand the development of STs. Data analysis has shown the role of climate on the morphological development of SW Iberia. Many processes, such as those linked with prior ST shaping could start in Cenozoic times, although glacio-eustatism drives later bedrock incision on the Variscan basement. The studied area represents an intraplate domain close to the boundary of the Iberian and African plates, active since Late Cretaceous. Our geomorphological and structural analysis helps to build a consistent geological history of Lower Guadiana River and to encourage bedrock river evolution studies on older intraplate domains.

## Acknowledgements

This study was financial supported by project CGL2011-28357 (MINECO, Spain). Useful manuscript suggestions were provided by Ellen Wohl. Ana Burton offered linguistic assistance. We wish to thank M. Stokes and another reviewer for their critical comments and insightful suggestions to clarify and improve the manuscript, and also acknowledge the editor Prof. Lecce Scott for his carefully corrections and remarks.

## References

Ábalos, B., Carreras, J., Druguet, E., Escuder Viruete, J., Gómez Pugnaire, M.T., Lorenzo Álvarez, S., Quesada, C., Rodríguez Fernández, L.R., Gil-Ibarguchi, I., 2002. Variscan and Pre-Varisvan Tectonics. In: Gibbons, W., Moreno, T. (Eds.), Geology of Spain. The Geological Society Pub., pp. 155–183.

Anton, L., Mather, A.E., Stokes, M., Munoz-Martin, A., De Vicente, G., 2015. Exceptional river gorge formation from unexceptional floods. Nat. Commun. 6, 7963.

Baker, V.R., Kale, V.S., 1998. The role of extreme floods in shaping bedrock channels. In: Tinkler, K.J., Wohl, E.E. (Eds.), Rivers over Rock: Fluvial Processes in Bedrock Channels. American Geophysical Union, Washington DC, pp. 153–165.

Boski, T., Moura, D., Veiga-Pires, C., Camacho, S., Duarte, D., Scott, D.B., Fernandes, S.G., 2002. Postglacial sea-level rise and sedimentary response in the Guadiana Estuary, Portugal/Spain border. Sediment. Geol. 150, 103–122.

Bridgland, D., Westaway, R., 2008. Climatically controlled river terrace staircases: a worldwide Quaternary phenomenon. Geomorphology 98, 285–315.

Brum da Silveira, A., Cabral, J., Perea, H., Ribeiro, A., 2009. Evidence for coupled reverse and normal active faulting in W Iberia. The Vidigueira–Moura and Alqueva faults (SE Portugal). Tectonophysics 474, 184–199.

Bucher, W.H., 1932. 'Strath' as a geomorphic term. Science 75,130–131. https://doi.org/10.1126/science.75.1935.130-a.

Bull, W.B., 1990. Stream-terrace genesis: implications for soil development. Geomorphology 3,351–367. https://doi.org/10.1016/0169-555X (90)90011-E.

Cabral, J., Mendes, Virgílio Brito, Figueiredo, P., Brum da Silveira, A., Pagarete, J., Ribeiro, A., Dias, R., Ressurreição, R., 2017. Active tectonics in Southern Portugal (SW Iberia) inferred from GPS data. Implications on the regional geodynamics. J. Geodyn. 112,1–11. https://doi.org/10.1016/j.jog.2017.10.002.

Cheng, S., Deng, Q., Zhou, S., Yang, G., 2002. Strath terraces of Jinshaan Canyon, Yellow River, and Quaternary tectonic movements of the Ordos Plateau, North China. Terra Nova 14, 215–224.

Collins, B.D., Montgomery, D.R., Schanz, S.A., Larsen, I.J., 2016. Rates and mechanisms of bedrock incision and strath terrace formation in a forested catchment, Cascade Range, Washington. Geol. Soc. Am. Bull. 128,926–943. https://doi.org/10.1130/B31340.1.

Cunha, P., Martins, A., Daveau, S., Friend, P., 2005. Tectonic control of the Tejo river fluvial incision during the late Cenozoic, in Ródão - central Portugal (Atlantic Iberian border). Geomorphology 64, 271–298.

Cunha, P.P., Martins, A.A., Gouveia, M.P., 2016. The terrace staircases of the Lower Tagus River (Ródão to Chamusca) characterization and interpretation of the sedimentary, tectonic, climatic and Palaeolithic data. Quatern. Stud. 14, 1–24.

Custódio, S., Dias, N.A., Carrilho, F., Góngora, E., Rio, I., Marreiros, C., Morais, I., Alves, P., Matias, L., 2015. Earthquakes in western Iberia: improving the understanding of lithospheric deformation in a slowly deforming region. Geophys. J. Int. 203,127–145. https://doi.org/10.1093/gji/ggv285.

Feio, M., 1946. Os Terraços do Guadiana a jusante do Ardila. Centro de Estudios Geográficos, Lisboa (in Portugese).

Feio, M., 1992. Geomorfología. In: Oliveira, J.T. (Ed.), Carta Geológica de Portugal: noticia explicativa de folha 8, escala 1/200000. Serviços Geológicos de Portugal, Lisboa, pp. 11–15 (in Portugese).

Finnegan, N.J., Dietrich, W.E., 2011. Episodic bedrock strath terrace formation due to meander migration and cutoff. Geology 39,143–146. https://doi.org/10.1130/G31716.1.

Fuller, T.K., Perg, L.A., Willenbring, J.K., Lepper, K., 2009. Field evidence for climate-driven changes in sediment supply leading to strath terrace formation. Geology 37,467–470. https://doi.org/10.1130/G25487A.1.

Garcia, A.F., 2006. Thresholds of strath genesis deduced from landscape response to stream piracy by Pancho Rico Creek in the Coast Ranges of central California. Am. J. Sci. 306,655–681. https://doi.org/10.2475/08.2006.03.

Garzón, G., Tejero, R., 2018. Las terrazas de las cuencas cenozoicas de Extremadura: Aportaciones de la luminiscencia. XV Reunión Nacional de Geomorfología, Mallorca (in press). (in Spanish).

Garzón, G., Ortega, J.A., Garrote, J., 2008. Morfología de perfiles de ríos en roca. Control tectónico y significado evolutivo en el Bajo Guadiana. Geogaceta 44, 63–66.

Garzón, G., Fernández, P., Pellicer, M.J., Babin, R., Tejero, R., 2011. Dataciones preliminares y arquitectura de las terrazas de la depresión de Badajoz (Vegas del Guadiana). In: y Constante, Turu (Ed.), El cuaternario en España y áreas afines, Avances en 2011, pp. 63–68 (in Spanish).
Garzón, G., Heydt, M.G., Ortega, J.A., Tejero, R., Meriaux, A.S., 2016. Bedrock river incision and strath terrace evolution: new insights in Lower Guadiana Canyon. In: Baryshnikov, G., Panin, A. (Eds.), Gradualism vs Catastrophism in Landscape Evolution. Altai State University, Barnaul, Russia, pp. 155–157.
Gilbert, G.K., 1877. Geology of the Henry Mountains. Government Printing Office, Washington, DC.
Goode, J.R., Wohl, E., 2010. Coarse sediment transport in a bedrock channel with complex bed topography. Water Resour. Res. 46 (W11524). https://doi.org/10.1029/2009WR008135.
Hancock, G.S., Anderson, R.S., 2002. Numerical modeling of fluvial strath-terrace formation in response to oscillating climate. Geol. Soc. Am. Bull. 114,1131–1142. https://doi.org/10.1130/0016-7606 (2002)114<1131:NMOFST>2.0.CO;2.
Hancock, G.S., Anderson, R.S., Whipple, K.X., 1998. Beyond power: bedrock river incision process and form. In: Tinkler, K.J., Wohl, E.E. (Eds.), Rivers over Rock: Fluvial Processes in Bedrock Channels. American Geophysical Union, Washington, DC, pp. 35–60.
Haq, B.U., Hardenbol, J., Vail, P.R., 1987. Chronology of fluctuating sea levels since the Triassic. Science 235, 1156–1167.
Harden, D.R., Coleman, S.M., 1988. Geomorphic and Quaternary history of Canyonlands, southeastern Utah. In: Holden, G.S. (Ed.), Geological Society of America Field Trip Guidebook Professional Contributions of Colorado School of Mines. Geological Society of America, Boulder, Colorado, pp. 336–369.
Johnson, K.N., Finnegan, N.J., 2015. A lithologic control on active meandering in bedrock channels. Geol. Soc. Am. Bull. 127,1766–1776. https://doi.org/10.1130/B31184.1.
Kale, V.S., 2003. Geomorphic effects of monsoon floods on Indian rivers. Nat. Hazards 28, 65–84.
Leopold, L.B., Miller, J.P., 1954. A postglaciar chronology of some alluvial valleys in Wyoming. U.S. Geol. Surv. Water-Supply Paper 1261, p. 90.
Leyva, F., Ramírez, J., 1983. Mapa Geológico de España 1:50.000. Hoja de Ayamonte n° 998. IGME, Madrid, Spain (in Spanish).
Lobo, F.J., Hernández-Molina, F.J., Somoza, L., Diaz de Río, V., 2001. The sedimentary record of the post-glacial transgression on the Gulf of Cádiz continental shelf (Southwest Spain). Mar. Geol. 178, 171–195.
Lobo, F.J., Dias, J.M.A., González, R., Hernández-Molina, F.J., Morales, J.A., Diaz de Río, V., 2003. High-resolution seismic stratigraphy of a narrow, bedrock-controlled estuary: the Guadiana estuarine system, SW Iberia. J. Sediment. Res. 73, 973–986.
Lourens, L.J., Antonarakau, A., Hilgen, F.J., Van Hoof, A.A.M., Vergnaud-Grazzini, C., Zachariasse, W.J., 1996. Evaluation of the Plio-Pleistocene astronomical timescale. Paleoceanography 11, 391–413.
Mackin, J.H., 1937. Erosional history of the Big Horn Basin, Wyoming. Geol. Soc. Am. Bull. 48,813–894. https://doi.org/10.1130/GSAB-48-813.
Martins, A., Cabral, J., Cunha, P., Stokes, M., Borgese, J., Caldeira, B.A., Cardoso Martins, A., 2017. Tectonic and lithological controls on fluvial landscape development in central-eastern Portugal: insights from long profile tributary stream analyses. Geomorphology 276, 44–163.
Merritts, D.J., Vincent, K.R., Wohl, E.E., 1994. Long river profiles, tectonism, and eustasy: a guide to interpreting fluvial terraces. J. Geophys. Res. Solid Earth 99,14,031–14,050. https://doi.org/10.1029/94JB00857.
Miller, K.G., Kominz, M.A., Browning, J.V., Wright, J.D., Mountain, G.S., Katz, M.E., Sugarman, P.J., Cramer, B.S., Christie-Blick, N., Pekar, S.F., 2005. The Phanerozoic record of global sea-level change. Science 310, 1293–1298.
Montgomery, D.R., 2004. Observations on the role of lithology in strath terrace formation and bedrock channel width. Am. J. Sci. 304,454–476. https://doi.org/10.2475/ajs.304.5.454.
Morales, J.A., 1997. Evolution and facies architecture of the mesotidal Guadiana River delta (SW Spain-Portugal). Mar. Geol. 138 (1–2), 127–148.
Niedzielski, T., Migon, P., Placek, A., 2009. A minimum sample size required from Schmidt hammer measurements. Earth Surf. Process. Landf. 34, 1713–1725.
Oliveira, J.T. (Ed.), 1992. Carta geológica de Portugal: noticia explicativa de folha 8, escala 1/200000. Serviços Geológicos de Portugal, Lisboa.
Ortega, J.A., 2007. Paleocrecidas, avenidas recientes e hidroclimatología en la cuenca media y baja del río Guadiana. (Ph.D. thesis). Universidad Complutense de Madrid, Spain (535 pp in Spanish).
Ortega, J.A., Garzón, G., 2009. A contribution to improved flood magnitude estimation in base of palaeoflood record and climatic implications–Guadiana River (Iberian Peninsula). Nat. Hazards Earth Syst. Sci. 9, 229–239.
Ouimet, W.B., Whipple, K.X., Royden, L.H., Sun, Z., Chen, Z., 2008. The influence of large landslides on river incision in a transient landscape: eastern margin of the Tibetan Plateau (Sichuan, China). Geol. Soc. Am. Bull. 119,1462–1476. https://doi.org/10.1130/B26136.1.
Pais, J., Cunha, P.P., Pereira, D., Legoinha, P., Dias, R., Moura, D., Brum, A., 2012. The Paleogene and Neogene of Western Iberia (Portugal). Springer.
Pazzaglia, F.J., Gardner, T.W., 1993. Fluvial terraces of the lower Susquehanna River. Geomorphology 8,83–113. https://doi.org/10.1016/0169-555X(93)90031-V.
Pazzaglia, F.J., Gardner, T.W., Merritts, D., 1998. Bedrock fluvial incision and longitudinal profile development over geologic time scales determined by fluvial terraces. In: Tinkler, K.J., Wohl, E.E. (Eds.), Rivers Over Rock: Fluvial Processes in Bedrock Channels. American Geophysical Union, Washington, DC, pp. 207–235.
Personius, S.F., Kelsey, H.M., Grabau, P.C., 1993. Evidence for regional stream aggradation in the central Oregon Coast Range during the Pleistocene-Holocene transition. Quat. Res. 40,297–308. https://doi.org/10.1006/qres.1993.1083.
Pitty, A.F., 1971. Introduction to Geomorphology. Methuen, London (526 p.).
Pratt, B., Burbank, D.W., Heimsath, A., Ojha, T., 2002. Impulsive alluviation during early Holocene strengthened monsoons, central Nepal Himalaya. Geology 30, 911–914.
Rodríguez-Vidal, J., Cáceres, L.M., Rodríguez-Ramírez, A., 1993. Modelo evolutivo de la red Fluvial Cuaternaria en el Suroeste de la Península Ibérica. 3ª Reunión do Quaternario Ibérico, Coimbra, pp. 33–38 (in Spanish).
Salazar, A., Larrasoaña, J.C., Abad, M., Mayoral, E., Pérez-Asensio, J.N., González-Regalado, M.L., Martín-Banda, R., Civis, J., Mata, M.P., 2016. Neogene lithological units at the west end of the Guadalquivir Basin and their correlations with the Huelva-1 borehole (Huelva-Spain). IX Congreso Geológico de España, Huelva. Geo-Temas 16, 177–180.
Santisteban, J.I., Schulte, L., 2007. Fluvial networks of the Iberian Peninsula: a chronological framework. Quat. Sci. Rev. 26, 22–24.
Schanz, S.A., Montgomery, D.R., 2016. Lithologic controls on valley width and strath terrace formation. Geomorphology 258, 58–68.
Seidl, M.A., Finkel, R.C., Caffee, M.V., Hudson, G.B., Dietrich, W.E., 1997. Cosmogenic isotope analysis applied to river longitudinal profile evolution: problems and interpretations. Earth Surf. Process. Landf. 22, 195–209.
Selby, M.J., 1980. A rock mass strength classification for geomorphic purposes: with tests from Antarctica and New Zealand. Z. Geomorphol. 24, 31–51.
Shackelton, N.J., 1987. Oxygen isotopes, ice volume and sea level. Quat. Sci. Rev. 6, 351–364.
Shepherd, R.G., Schumm, S.A., 1974. Experimental study of river incision. GSA Bull. 85, 257–268.
Stokes, M., Mather, A.E., Belfoul, M., Faik, F., Bouzid, S., Geach, M.R., Cunha, P.P., Boulton, S.J., Thiel, C., 2017. Controls on dryland mountain landscape development along the NW Saharan desert margin: insights from Quaternary river terrace sequences (Dades River, south-central High Atlas, Morocco). Quat. Sci. Rev. 166, 363–379.
Terrinha, P., Rocha, R., Rey, J., Cachão, M., Moura, D., Roque, C., Martins, L., Valadares, V., Cabral, J., Azevedo, M.R., Barbero, L., Clavijo, E., Días, R.P., Gafeira, Matias, H., Madeira, J., Marques da Silva, C., Munhá, J., Rebelo, L., Ribeiro, C., Vicente, J., Youbi, N., 2006. A Bacia do Algarve; estratigrafía, paleogeografía e tectónica. In: Dias, R., Araújo, A., Terrinha, P., Kullberg, J.C. (Eds.), Geología de Portugal no contexto da Ibéria. Univ. Évora, Évora, Portugal, pp. 247–316 (in Portuguese).
Tooth, S., 2015. The Augrabies Falls Region: a fluvial landscape divided in flow but magnificent in spectacle. In: Grab, S., Knight, J. (Eds.), Landscapes and Landforms of South Africa. Springer,pp. 65–73 https://doi.org/10.1007/978-3-319-03560-4_8.
Vázquez-Vílchez, M., Jabaloy-Sánchez, A., Azor, A., Stuart, F., Persano, C., Alonso-Chaves, F.M., Martín-Parra, L.M., Matas, J., García-Navarro, E., 2015. Mesozoic and Cenozoic exhumation history of the SW Iberian Variscides inferred from low-temperature thermochronology. Tectonophysics 663, 110–121.
Ward, D.J., Spotila, J.A., Hancock, G.S., Galbraith, J.M., 2005. New constraints on the late Cenozoic incision history of the New River, Virginia. Geomorphology 72,54–72. https://doi.org/10.1016/j.geomorph.2005.05.002.
Wegmann, K.W., Pazzaglia, F.J., 2002. Holocene strath terraces, climate change, and active tectonics: the Clearwater River basin, Olympic Peninsula, Washington State. Geol. Soc. Am. Bull. 114,731–744. https://doi.org/10.1130/0016-7606 (2002)114<0731:HSTCCA>2.0.CO;2.
Whipple, K.X., 2004. Bedrock rivers and the geomorphology of active orogens. Annu. Rev. Earth Planet. Sci. 32, 151–185.
Whipple, K.X., Hancock, G.S., Anderson, R.S., 2000. River incision into bedrock: mechanics and relative efficacy of plucking, abrasion, and cavitation. Geol. Soc. Am. Bull. 112, 490–503.
Wohl, E.E., 2008. The effect of bedrock jointing on the formation of straths in the Cache la Poudre drainage, Colorado Front Range. J. Geophys. Res. 113, F01007. https://doi.org/10.1029/2007JF000817.
Wohl, E.E., Thompson, D.M., Miller, A.J., 1999. Canyons with undulating walls. Geol. Soc. Am. Bull. 111, 949–959.
Wolanski, E., Chicharo, L., Chicharo, M.A., Morais, P., 2006. An ecohydrology model of the Guadiana Estuary (South Portugal). Estuar. Coast. Shelf Sci. 70, 132–143.